COMPARISON OF LOCALIZED, INTERLEAVED AND BLOCK-INTERLEAVED FDMA IN TERMS OF PILOT MULTIPLEXING AND CHANNEL ESTIMATION

Anja Sohl and Anja Klein

Darmstadt University of Technology
Communications Engineering Lab
Merckstr. 25, 64283 Darmstadt, Germany
a.sohl@nt.tu-darmstadt.de

ABSTRACT

In this paper, DFT-precoded OFDMA is compared in terms of pilot assisted channel estimation in frequency domain for an uplink scenario considering the three different ways of subcarrier allocation: localized, interleaved and block-interleaved. The feasibility of different methods of pilot multiplexing is investigated for the three possibilities, as well as the influence of pilot multiplexing on the Peak-to-Average Power Ratio, the pilot symbol overhead and the channel estimation performance. Further on, the practicability of a post processing algorithm, which is applied to the estimated channel impulse response, is considered for localized, interleaved and block-interleaved subcarrier allocation.

1. INTRODUCTION

At present, research activities for beyond 3rd generation of mobile radio systems are in progress worldwide. For the uplink, several multiple access (MA) schemes are under discussion as candidates, as e.g. Orthogonal Frequency Division Multiple Access (OFDMA) because of its favorable properties as they have been described in [13]. Other promising MA schemes result from the application of Discrete Fourier Transform (DFT) precoding to OFDMA. OFDMA with DFT precoding combines the advantages of OFDMA with a low Peak-to-Average Power Ratio (PAPR) of the transmit signal [6]. For DFT precoded OFDMA, there exist different possibilities of how to allocate subcarriers to a specific user.

A blockwise allocation of subcarriers leads to a MA scheme that is well known as Localized Frequency Division Multiple Access (LFDMA) [12]. Due to the blockwise structure, LFDMA provides good robustness to carrier frequency offsets as well as high multi user diversity gains in case of adaptive resource allocation [7]. In terms of channel estimation (CE) in frequency domain (FD), LFDMA provides the possibility of interpolation between subcarriers allocated to a specific user. On the other hand, LFDMA shows low frequency diversity because the subcarriers allocated to a specific user are restricted to a localized fraction of the available bandwidth [8]. Further on, the PAPR reduction is less significant than for other DFT-precoded OFDMA systems.

As a second possibility of subcarrier allocation, a set of equidistant subcarriers that are distributed over the available bandwidth is assigned to each user. This subcarrier structure leads to the Interleaved Frequency Division Multiple Access (IFDMA) scheme [10], [5]. Due to the distributed subcarriers, IFDMA provides high frequency diversity [3]. Further on, there exists a very efficient implementation for signal generation in time domain (TD) for IFDMA, which is beneficial for implementation in the mobile terminal [5]. Compared to other DFT-precoded OFDMA schemes, IFDMA provides the lowest PAPR and, thus, enables the application of low cost amplifiers. On the other hand, IFDMA is sensitive against carrier frequency offsets [4]. Moreover, in terms of CE for IFDMA, in general, interpolation in FD between different subcarriers allocated to a specific user is not possible.

A third possibility of subcarrier allocation is currently under investigation and denoted as Block IFDMA (B-IFDMA) [15]. Here, the data of a specific user is transmitted on blocks of subcarriers that are equidistantly distributed over the available bandwidth. In contrast to IFDMA, where a block is built by a single subcarrier, for B-IFDMA, each block consists of K_f adjacent subcarriers. Due to the blockwise allocation, B-IFDMA is assumed to exhibit higher robustness against carrier frequency offsets than IFDMA and, at the same time, maintain the advantage of high frequency diversity. In terms of CE, another advantageous aspect of B-IFDMA compared to IFDMA is the support of interpolation in FD within each block of K_f subcarriers.

Thus, different possibilities of subcarrier allocation lead to different characteristics of the resulting MA scheme. In this paper, a comparison of LFDMA, IFDMA and B-IFDMA in terms of pilot multiplexing and channel estimation will be given for an uplink scenario. The focus will be on different possibilities of pilot insertion that are dependent on the applicability of interpolation. For each possibility of pilot insertion, the three MA schemes will be compared in terms of feasibility, PAPR of the transmitted signal, the overhead that has to be spent for pilot symbols and CE performance. Further on, a post processing (PP) algorithm can be applied for further improvement of CE performance. The influence of pilot insertion on the PP gain will be investigated.

The paper is organized as follows. In section 2, the system model is described. In section 3, techniques of pilot insertion are proposed for LFDMA, IFDMA and B-IFDMA. In section 4, CE is described for the different proposals of pilot insertion for LFDMA, IFDMA and B-IFDMA. Section 5 comprises calculation and results of pilot symbol overhead. In section 6, results for CE performance with and without PP are discussed. Section 7 concludes the work.

2. SYSTEM MODEL

In this section, a system model for LFDMA, IFDMA and B-IFDMA will be derived from the general description of the DFT-precoded OFDMA system model.

In the following, all signals are represented by their discrete time equivalents in the complex baseband. Further on, $(\cdot)^T$ denotes the transpose and $(\cdot)^H$ the Hermitian of a vector or a matrix. Assuming a system with K users, let $\mathbf{d}^{(k)} = (d_0^{(k)}, \cdots, d_{Q-1}^{(k)})^T$ denote a block of Q data symbols $d_q^{(k)}, q = 0, \cdots, Q-1$, at symbol rate $1/T_s$ transmitted by a user with index k, $k = 0, \cdots, K-1$. The data symbols $d_q^{(k)}$ can be taken from the alphabet of a modulation scheme like Phase Shift Keying (PSK), that is applied to coded or uncoded bits. Let $\mathbf{F}_N$ and $\mathbf{F}_N^H$ denote the matrix representation of an N-point DFT and an N-point Inverse DFT (IDFT) matrix, respectively, where $N = K \cdot Q$ is the number of available subcarriers in the system.

The assignment of the data symbols $d_q^{(k)}$ to the user specific set of Q subcarriers can be described by a Q-point DFT precoding matrix $\mathbf{F}_Q$, an $N \times Q$ mapping matrix $\mathbf{M}^{(k)}$ and an N-point IDFT matrix $\mathbf{F}_N^H$ [3]. Thus, a DFT-precoded OFDMA symbol with elements at chip rate $1/T_c = K/T_S$ is given by

$$\mathbf{x}^{(k)} = \mathbf{F}_N^H \cdot \mathbf{M}^{(k)} \cdot \mathbf{F}_Q \cdot \mathbf{d}^{(k)}. \quad (1)$$

The insertion of a Cyclic Prefix, as well as the transmission over a channel and subsequent demodulation is given in [3] and will not be described in this work.

2.1 LFDMA

A system model for LFDMA can be derived as a special case of the DFT-precoded OFDMA system model with blockwise subcarrier allocation. The elements $M_L^{(k)}(n,q)$ with $n = 0,\cdots,N-1$ and $q = 0,\cdots,Q-1$ of the mapping matrix $\mathbf{M}_L^{(k)}$ are given by

$$M_L^{(k)}(n,q) = \begin{cases} 1 & n = k\cdot Q+q \\ 0 & \text{else} \end{cases} . \quad (2)$$

Thus, the LFDMA transmit signal $\mathbf{x}_L^{(k)}$ becomes

$$\mathbf{x}_L^{(k)} = \mathbf{F}_N^H \cdot \mathbf{M}_L^{(k)} \cdot \mathbf{F}_Q \cdot \mathbf{d}^{(k)}. \quad (3)$$

2.2 IFDMA

To derive a system model for IFDMA as a special case of the introduced DFT-precoded OFDMA system model, the mapping matrix has to perform an interleaved subcarrier allocation. The IFDMA mapping matrix $\mathbf{M}_I^{(k)}$ is given by its elements $M_I^{(k)}(n,q)$, with $n = 0,\cdots,N-1$, and $q = 0,\cdots,Q-1$.

$$M_I^{(k)}(n,q) = \begin{cases} 1 & n = q\cdot K+k \\ 0 & \text{else} \end{cases} . \quad (4)$$

Thus, the IFDMA transmit signal $\mathbf{x}_I^{(k)}$ becomes

$$\mathbf{x}_I^{(k)} = \mathbf{F}_N^H \cdot \mathbf{M}_I^{(k)} \cdot \mathbf{F}_Q \cdot \mathbf{d}^{(k)}. \quad (5)$$

2.3 B-IFDMA

The signal generation for B-IFDMA can be described in two different ways. First, as an assignment of multiple IFDMA signals to one user and second, as one joint DFT for all subcarriers assigned to a user. As the second methods exhibits a lower PAPR than the first [9], we will concentrate on the second method of signal generation in this paper. In the following, K_f denotes the number of subcarriers per block and T denotes the number of blocks assigned to a specific user k, with $Q = K_f \cdot T$. For B-IFDMA, the mapping matrix has to characterize a block interleaved subcarrier allocation. The B-IFDMA mapping matrix $\mathbf{M}_B^{(k)}$ is given by its elements $M_B^{(k)}(n,q)$,

$$M_B^{(k)}(n, q = t\cdot K_f + r) = \begin{cases} 1 & n = t\cdot\frac{N}{T} + r + k\cdot K_f \\ 0 & \text{else} \end{cases} , \quad (6)$$

with $n = 0,\cdots,N-1$, $r = 0,...,K_f-1$ and $t = 0,...,T-1$. Thus, the B-IFDMA transmit signal $\mathbf{x}_B^{(k)}$ of user k becomes

$$\mathbf{x}_B^{(k)} = \mathbf{F}_N^H \cdot \mathbf{M}_B^{(k)} \cdot \mathbf{F}_Q \cdot \mathbf{d}^{(k)}. \quad (7)$$

In Fig. 1, the subcarrier allocation of LFDMA, IFDMA and B-IFDMA is depicted for an exemplary set of parameters.

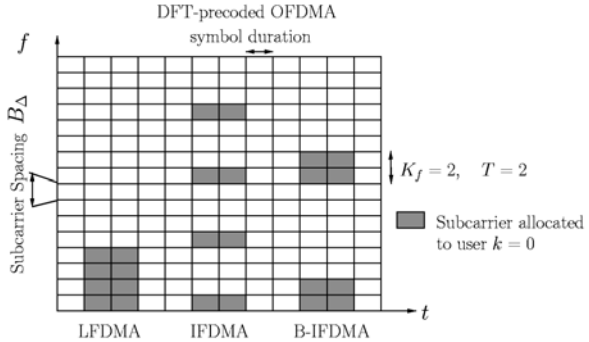

Figure 1: Exemplary subcarrier allocation for LFDMA, IFDMA, B-IFDMA with $N = 16$, $Q = 4$ and for user $k = 0$

3. PILOT INSERTION

In this section, two different possibilities of pilot insertion are investigated for LFDMA, IFDMA and B-IFDMA. First, a DFT-precoded OFDMA symbol is used to transmit a pilot sequence (PS) on each subcarrier allocated to a certain user. This method is termed symbolwise pilot insertion in the following. In order to reduce pilot symbol overhead, it is beneficial to interpolate between adjacent subcarriers assigned to a user k. Therefore, a second method of pilot insertion is introduced in which the pilots are transmitted only on a certain subset of the total number of subcarriers assigned to user k in one symbol. This method is termed subcarrierwise pilot insertion in the following.

3.1 Symbolwise Pilot Insertion

For symbolwise pilot insertion, an appropriate PS $\tilde{\mathbf{p}}^{(k)} = (\tilde{p}_0^{(k)},\cdots,\tilde{p}_{Q-1}^{(k)})^T$ is transmitted within one DFT-precoded OFDMA symbol. In FD this means that pilots are transmitted on each subcarrier allocated to a certain user and that no data is transmitted within this symbol. The unmodulated PS $\tilde{\mathbf{p}}^{(k)}$ consists of Q complex values, as, e.g., elements of a Constant Amplitude Zero Autocorrelation (CAZAC) sequence [1]. In order to maintain the orthogonality of the K users' signals, the PS $\tilde{\mathbf{p}}^{(k)}$ is modulated in analogy to the particular signal model for LFDMA, IFDMA and B-IFDMA. The application of the mapping matrix $\mathbf{M}_{L/I/B}^{(k)}$ for LFDMA, IFDMA and B-IFDMA given in section 2.1, 2.2 and 2.3 leads to the PS generation of the particular MA scheme.

Thus, the PS $\mathbf{p}_{L/I/B}^{(k)}$ for LFDMA, IFDMA and B-IFDMA is given by

$$\mathbf{p}_{L/I/B}^{(k)} = \mathbf{F}_N^H \cdot \mathbf{M}_{L/I/B}^{(k)} \cdot \mathbf{F}_Q \cdot \tilde{\mathbf{p}}^{(k)}. \quad (8)$$

For all three schemes, the sequence $\mathbf{x}^{(k)}$ transmitted in TD for CE is given by $\mathbf{x}_{L/I/B}^{(k)} = \mathbf{p}_{L/I/B}^{(k)}$. The FD representation of the modulated PS $\mathbf{p}_{L/I/B}^{(k)}$ of user k is given by its N-point DFT

$$\mathbf{P}_{L/I/B}^{(k)} = \mathbf{F}_N \cdot \mathbf{p}_{L/I/B}^{(k)} = (P_0^{(k)},\cdots,P_{N-1}^{(k)})^T. \quad (9)$$

For the three MA schemes, $\mathbf{P}_{L/I/B}^{(k)}$ exhibits different positions of the non-zero elements. The non-zero elements of $\mathbf{P}_{L/I/B}^{(k)}$ can be combined in a vector

$$\mathbf{P}_{sy}^{(k)} = (P_{sy,0}^{(k)},...,P_{sy,Q-1}^{(k)}) \quad (10)$$

with Q elements. For LFDMA, the elements $P_{sy,\hat{n}_L}^{(k)}$ of $\mathbf{P}_{sy}^{(k)}$ are given by $P_{sy,\hat{n}_L=q}^{(k)} = P_{k\cdot Q+q}^{(k)}$, with $q = 0,\cdots,Q-1$. For IFDMA, the elements $P_{sy,\hat{n}_I}^{(k)}$ of $\mathbf{P}_{sy}^{(k)}$ are given by $P_{sy,\hat{n}_I=q}^{(k)} = P_{q\cdot K+k}^{(k)}$, with $q = 0,\cdots,Q-1$. For B-IFDMA, the non-zero elements are given by $P_{sy,\hat{n}_B=(t\cdot K_f+r)}^{(k)} = P_{t\cdot N/T+r+k\cdot K_f}^{(k)}$, with $r = 0,\cdots,K_f-1$ and $t = 0,...,T-1$.

The PAPR of the data signal with pilots inserted symbolwise shows the same behaviour as the PAPR of the data signal itself for LFDMA, IFDMA or B-IFDMA modulation, respectively. Thus, the IFDMA signal exhibits the lowest PAPR, whereas the PAPR of LFDMA and B-IFDMA degrades compared to IFDMA.

3.2 Subcarrierwise Pilot Insertion

The subcarrierwise pilot insertion is performed by using N_p subcarriers of the total number Q of subcarriers allocated to a certain user for pilot transmission.The elements $\tilde{P}_p$, $p = 0,...,N_p-1$, of the DFT of a PS $\tilde{\mathbf{p}} = (p_0,\cdots,p_{N_p-1})$ with elements, e.g., taken from a

CAZAC sequence, are transmitted on the N_p subcarriers. N_p is dependent on the depth I_p of interpolation in FD, e.g., for $I_p = 2$ every 2nd subcarrier that is allocated to a specific user has to be used for pilot transmission. For simplicity, it is assumed that I_p is always chosen in that way to achieve an integer number N_p of pilots.

- *LFDMA*
  For LFDMA, the length of the PS $\tilde{\mathbf{p}}^{(k)}$ is given by $N_p = Q/I_p$. The transmitted PS $\mathbf{p}_L^{(k)}$ in TD is described by a modified IFDMA-modulation and thus,

$$\mathbf{p}_L^{(k)} = \mathbf{F}_N^H \cdot \mathbf{M}_{pL}^{(k)} \cdot \mathbf{F}_{N_p} \cdot \tilde{\mathbf{p}}^{(k)}. \tag{11}$$

  The elements of the mapping matrix $\mathbf{M}_{pL}^{(k)}$ are given by

$$M_{pL}^{(k)}(n, q_p) = \begin{cases} 1 & n = q_p \cdot I_p + k \cdot Q \\ 0 & \text{else} \end{cases}, \tag{12}$$

  with $q_p = 0, \cdots, N_p - 1$ and $n = 0, \cdots, N-1$.
  Within this block of pilot transmission, $Q - N_p$ subcarriers are not used for pilot transmission and, thus, a data sequence (DS) $\tilde{\mathbf{d}}^{(k)} = (d_0, ..., d_{Q-N_p-1})$ can be transmitted. $\tilde{\mathbf{d}}^{(k)}$ is modulated according to

$$\mathbf{d}_L^{(k)} = \mathbf{F}_N^H \cdot \mathbf{M}_{dL}^{(k)} \cdot \mathbf{F}_{Q-N_p} \cdot \tilde{\mathbf{d}}^{(k)}. \tag{13}$$

  The elements $M_{dL}^{(k)}(n, q_d)$ with $n = 0, ..., N-1$ and $q_d = t \cdot I_p + p$ of the mapping matrix $\mathbf{M}_{dL}^{(k)}$ are given by

$$M_{dL}^{(k)}(n, t \cdot I_p + p) = \begin{cases} 1 & n = t \cdot I_p + p + k \cdot Q \\ 0 & \text{else} \end{cases}, \tag{14}$$

  with $t = 0, ..., N_p - 1$ and $p = 1, ..., I_p - 1$.
- *IFDMA*
  For IFDMA, $N_p = Q/I_p$. The transmitted PS $\mathbf{p}_I^{(k)}$ is given by

$$\mathbf{p}_I^{(k)} = \mathbf{F}_N^H \cdot \mathbf{M}_{pI}^{(k)} \cdot \mathbf{F}_{N_p} \cdot \tilde{\mathbf{p}}^{(k)}, \tag{15}$$

  with the elements $M_{pI}^{(k)}(n, q_p)$ for $n = 0, ..., N-1$ and $q_p = 0, ..., N_p - 1$ of the mapping matrix $\mathbf{M}_{pI}^{(k)}$

$$M_{pI}^{(k)}(n, q_p) = \begin{cases} 1 & n = q_p \cdot K \cdot I_p + k \\ 0 & \text{else} \end{cases}. \tag{16}$$

  The DS $\tilde{\mathbf{d}}^{(k)} = (d_o, ..., d_{Q-N_p-1})$ transmitted in the same block is divided into $(Q - N_p)/N_p$ subblocks with $\bar{\mathbf{d}}^{(m,k)}$ the m-th N_p elementary subblock of $\tilde{\mathbf{d}}$ with elements $d_{q_d}^{(m,k)} = d_{mN_p+q_d}^{(k)}$; $q_d = 0, ..., N_p - 1$ and $m = 0, ..., I_p - 2$. The modulated DS is given by

$$\mathbf{d}_I^{(k)} = \sum_{m=0}^{I_p-2} \mathbf{F}_N^H \cdot \mathbf{M}_{dI}^{(m,k)} \cdot \mathbf{F}_{N_p} \cdot \bar{\mathbf{d}}^{(m,k)}, \tag{17}$$

  with the elements of the mapping matrix $\mathbf{M}_{dI}^{(m,k)}$ given by

$$M_{dI}^{(m,k)}(n, q_d) = \begin{cases} 1 & n = q_d \cdot K \cdot I_p + k + (m+1) \cdot K \\ 0 & \text{else} \end{cases} \tag{18}$$

  for $n = 0, ..., N-1$.

- *B-IFDMA*
  For B-IFDMA, $N_p = T$ and the transmitted PS $\mathbf{p}_B^{(k)}$ is given by

$$\mathbf{p}_B^{(k)} = \mathbf{F}_N^H \cdot \mathbf{M}_{pB}^{(k)} \cdot \mathbf{F}_{N_p} \cdot \tilde{\mathbf{p}}^{(k)}, \tag{19}$$

  with T and K_f as defined in section 2.3. The elements of the mapping matrix $\mathbf{M}_{pB}^{(k)}$ are given by

$$M_{pB}^{(k)}(n, q_p) = \begin{cases} 1 & n = t \cdot \frac{N}{T} + p \cdot I_p + k \cdot K_f \\ 0 & \text{else} \end{cases}, \tag{20}$$

  for $n = 0, ..., N-1$, $q_p = p + t \cdot \frac{K_f}{I_p}$, $t = 0, ..., T-1$ and $p = 0, ..., \frac{K_f}{I_p} - 1$. The DS $\tilde{\mathbf{d}}^{(k)} = (d_o, ..., d_{Q-N_p-1})$ is mapped onto $Q - N_p$ remaining subcarriers. The transmitted DS $\mathbf{d}_B^{(k)}$ is given by

$$\mathbf{d}_B^{(k)} = \mathbf{F}_N^H \cdot \mathbf{M}_{dB}^{(m,k)} \cdot \mathbf{F}_{Q-N_p} \cdot \tilde{\mathbf{d}}^{(k)}, \tag{21}$$

  with the elements of the mapping matrix $\mathbf{M}_{dB}^{(k)}$ given by

$$M_{dB}^{(k)}(n, q_d) = \begin{cases} 1 & n = t \cdot \frac{N}{T} + r \cdot I_p + k \cdot K_f + b + 1 \\ 0 & \text{else} \end{cases} \tag{22}$$

  for $n = 0, ..., N-1$, $q_d = b + r \cdot (I_p - 1) + t \cdot \frac{K_f}{I_p}$ for $t = 0, ..., T-1$; $r = 0, ..., \frac{K_f}{I_p} - 1$ and $b = 0, ..., I_p - 2$.

For the three MA schemes, the non-zero elements of the N-point DFT $\mathbf{P}_{L/I/B}^{(k)}$ of $\mathbf{p}_{L/I/B}^{(k)}$ are combined in a vector

$$\mathbf{P}_{sc}^{(k)} = (P_{sc,0}^{(k)}, ..., P_{sc,N_p-1}^{(k)}) \tag{23}$$

with N_p elements. For LFDMA, the elements $P_{sc,\hat{n}_L}^{(k)}$ of $\mathbf{P}_{sc}^{(k)}$ are given by $P_{sc,\hat{n}_L=q_p}^{(k)} = P_{k \cdot Q + q_p \cdot I_p}^{(k)}$, with $q_p = 0, \cdots, N_p - 1$. For IFDMA, the elements $P_{sc,\hat{n}_I}^{(k)}$ of $\mathbf{P}_{sc}^{(k)}$ are given by $P_{sc,\hat{n}_I=q_p}^{(k)} = P_{q_p \cdot K \cdot I_p + k}^{(k)}$, with $q_p = 0, \cdots, N_p - 1$. For B-IFDMA, the non-zero elements are given by $P_{sc,\hat{n}_B=(t \cdot K_f/I_p + r)}^{(k)} = P_{t \cdot N/T + r \cdot I_p + k \cdot K_f}^{(k)}$, with $r = 0, \cdots, K_f/I_p - 1$ and $t = 0, ..., T-1$.

For all three schemes, the sequence $\mathbf{x}^{(k)}$ transmitted in TD for CE is given by the sum of pilot and data sequence and thus, $\mathbf{x}_{L/I/B}^{(k)} = \mathbf{d}_{L/I/B}^{(k)} + \mathbf{p}_{L/I/B}^{(k)}$.

As the sequence $\mathbf{x}_{L/I/B}^{(k)}$ transmitted for CE is built of a sum of several signals for LFDMA, IFDMA and B-IFDMA, the PAPR suffers for all three schemes due to constructive and destructive superpositions of the signals. Therefore, for subcarrierwise pilot insertion the PAPR degrades for all three schemes.

4. CHANNEL ESTIMATION

In this section, a channel estimation algorithm is proposed for LFDMA, IFDMA and B-IFDMA. In the following, only one user will be considered and the index k will be omitted for simplicity. Let $\mathbf{h} = (h_0, \cdots, h_{N-1})^T$ denote the vector representation of a channel with N coefficients h_i, $i = 0, \cdots, N-1$, at chip rate $1/T_c$, including L non-zero channel coefficients. The channel is assumed to be time invariant for the transmission of the PS. The values V_n with $n = 0, \cdots, N-1$, received on each subcarrier after transmission over the channel $\mathbf{h}$ can be described by one complex channel coefficient H_n due to flat fading on each subcarrier in FD and are given by

$$V_n = H_n \cdot P_n + \check{N}_n. \tag{24}$$

The values H_n denote the complex coefficients of the Channel Transfer Function (CTF) $\mathbf{H} = \mathbf{F}_N \cdot \mathbf{h} = (H_0, \cdots, H_{N-1})^T$ and $\breve{\mathbf{N}} = \mathbf{F}_N \cdot \breve{\mathbf{n}} = (\breve{N}_0, \cdots, \breve{N}_{N-1})^T$ denotes the Additive White Gaussian Noise (AWGN) on each subcarrier in FD. At the non-zero samples $P_{\hat{n}_{L/I/B}} = P_{\hat{n}}$ of the PS in FD, the channel transfer coefficients $H_{\hat{n}}$ can be estimated by

$$\hat{H}_{n_z} = \frac{V_{\hat{n}}}{P_{\hat{n}}} = H_{\hat{n}} + \frac{\breve{N}_{\hat{n}}}{P_{\hat{n}}} = H_{\hat{n}} + E_{\hat{n}}. \quad (25)$$

4.1 Symbolwise Pilot Insertion

For symbolwise pilot insertion, the vector of estimated channel transfer coefficients for LFDMA, IFDMA and B-IFDMA is given by

$$\hat{\mathbf{H}} = (\hat{H}_0, ..., \hat{H}_{Q-1}). \quad (26)$$

The symbolwise pilot insertion is always feasible for all three MA schemes, as the pilot symbols are transmitted on each subcarrier allocated to a specific user and therefore no interpolation is required.

4.2 Subcarrierwise Pilot Insertion

For subcarrierwise pilot insertion, it is assumed, that at least 5 pilots have to be transmitted within the coherence bandwidth B_k of the channel to fulfill the sampling theorem in FD. The vector $\hat{\mathbf{H}}$ of estimated channel transfer coefficients is given by

$$\hat{\mathbf{H}} = (\hat{H}_0, ..., \hat{H}_{N_p-1}). \quad (27)$$

An estimate for the channel transfer coefficients of each subcarrier allocated to the user under consideration is obtained by using interpolation. In-between neighboring pilot carrying subcarriers with a distance fulfilling the sampling theorem in FD, linear interpolation is applied. For subcarriers at the outer margin of such neighboring pilot carrying subcarriers, extrapolation is used. If there is only one pilot within the coherence bandwidth, the channel transfer coefficient is determined by repeating the coefficient of the pilot carrying subcarrier.

- *LFDMA*
  For LFDMA, interpolation is always possible if $Q > 1$, as the Q subcarriers allocated to a specific user are adjacent to each other.
- *IFDMA*
  For IFDMA, interpolation in FD is not possible as long as $5 \cdot K \cdot B_\Delta \geq B_k$ [8]. B_Δ denotes the subcarrier spacing. Thus, the subcarrierwise pilot insertion can only be applied to IFDMA in case of very high data rates.
- *B-IFDMA*
  For B-IFDMA, interpolation in FD can be applied within one block of K_f subcarriers if $K_f > 1$. This constraint is always valid for B-IFDMA as for $K_f = 1$ the modulation changes into the IFDMA scheme.

5. PILOT SYMBOL OVERHEAD

The overhead that occurs due to pilot transmission for CE can be described for all three MA schemes together. As the energy that has to be spent per data bit is increased relatively by pilot transmission, the overhead is equivalent to the Signal-to-Noise-Ratio (SNR)-degradation

$$\Lambda = 10 \cdot \log_{10}\left(\frac{Q \cdot N_S}{Q \cdot N_S - N_t \cdot N_f}\right), \quad (28)$$

[2], with N_f the number of required pilots in frequency direction and N_t the number of required pilots in time direction of Q overall symbols in frequency direction and N_S overall symbols in time direction, respectively.
For symbolwise pilot insertion, LFDMA, IFDMA and B-IFDMA exhibit the same pilot symbol overhead as one symbol is required for pilot transmission within the coherence time, respectively.
In the case of subcarrierwise pilot insertion, for LFDMA and B-IFDMA, there are always at least two adjacent subcarriers allocated to a certain user. Therefore, the subcarrierwise pilot insertion is always feasible and, thus, the pilot symbol overhead is decreased. As for IFDMA interpolation in FD is solely possible for high data rates, it exhibits a higher overhead for low and moderate data rates than LFDMA and B-IFDMA.

Table 1: Simulation Parameters

Carrier Frequency	3.7 GHz
Bandwidth	40 MHz
No. of Subcarriers	1024
Modulation	QPSK
Coding	Conv. Coding
Code Rate	1/2
Constraint Length	6
Decoder	MaxLogMAP
Equalizer	Linear MMSE FDE
Interleaving	Random
Interleaving Depth	0.5 ms
Guard Interval	3.6 μs
Channel	WINNER SCM [14]
Velocity	50 km/h

In Fig. 2, the pilot symbol overhead Λ in dB is given in dependency of the net bit rate in Mbit/s for the three schemes. The results are valid for the parameters in Table 1, a maximum channel delay of $\tau_{max} = 2.56\ \mu s$ and a maximum Doppler frequency of $f_{D,max} = 290$ Hz. One pilot symbol is transmitted per 24 symbols in time direction and one pilot per 2 adjacent subcarriers in frequency direction. The maximum velocity of the mobile is 62.5 km/h [8]. It can be seen that IFDMA exhibits an 0.09 dB higher overhead compared to LFDMA and B-IFDMA for net bit rates in-between 0.08 Mbit/s and 10 Mbit/s due to the missing interpolation in this range of data rate.

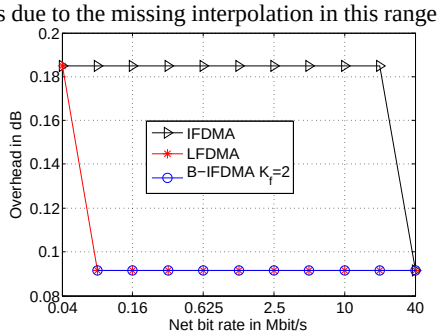

Figure 2: Pilot Symbol Overhead Λ

6. PERFORMANCE ANALYSIS

In this section, performance results are given for LFDMA, IFDMA and B-IFDMA. The performance results for data detection with realistic CE with symbol- and subcarrierwise pilot insertion are discussed for the three schemes. Additionally, results are shown with realistic CE and post processing (PP) applied in TD. The PP algorithm is applied to the estimated channel impulse response (CIR) by introducing a threshold and discarding every coefficient of the estimated CIR smaller than this threshold, because they are assumed to primarily consist of noise. The mathematical description of the PP algorithm has been given in [8] and [11] and will not be introduced in this work. The results are valid for the parameters given in Table 1. In Fig. 3-5, the coded BER performance of data detection with realistic CE with symbol- and subcarrierwise pilot insertion with and without application of PP is given. As the effect of CE solely is of interest in this work, the results are given for $Q = 512$ subcarriers per user which corresponds to a net bit rate of 20 Mbit/s where the three schemes show only slight difference in frequency diversity. The results for LFDMA are presented in Fig. 3, the results for IFDMA and B-IFDMA are presented in Fig. 4 and Fig. 5, respectively. The CE with symbolwise pilot insertion compared to perfect channel knowledge (PCK) exhibits an SNR-degradation of about 3 dB at a bit error rate of BER=10^{-3} for all three schemes. This

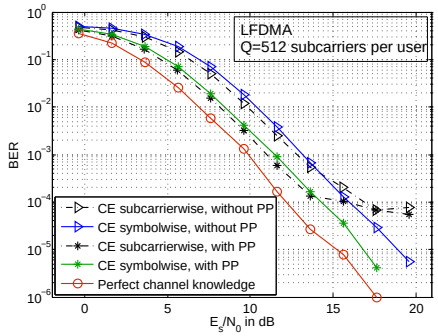

Figure 3: LFDMA with realistic CE

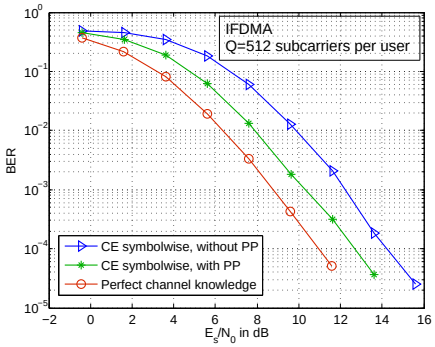

Figure 4: IFDMA with realistic CE

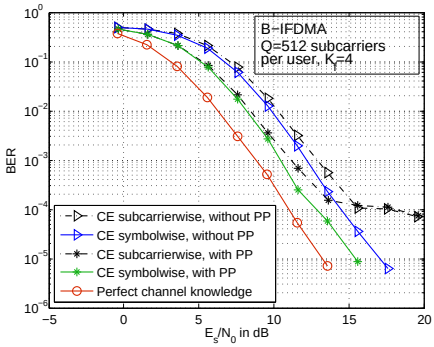

Figure 5: B-IFDMA with realistic CE

is also valid for any other data rate. For LFDMA and B-IFDMA, subcarrierwise pilot insertion can be applied, whereas this is not possible for IFDMA at this data rate of 20 Mbit/s. It can be seen, that the application of linear interpolation leads to a slightly lower BER for LFDMA in comparison to symbolwise pilot insertion for LFDMA and also in comparison to subcarrierwise pilot insertion for B-IFDMA. The linear interpolation for LFDMA leads to a slight noise mitigation for the channel coefficients of the interpolated subcarriers and therefore results in a better BER than for symbolwise pilot insertion at BER=10^{-3}. As for LFDMA the data is transmitted on Q adjacent subcarriers, only the channel coefficient of the last subcarrier in this block of Q subcarriers is determined by extrapolation, whereas for B-IFDMA extrapolation is used within each block of K_f adjacent subcarriers. Therefore, for subcarrierwise pilot insertion, LFDMA shows better results than B-IFDMA. It can also be seen that due to interpolation errors the BER degrades for increasing SNR for the subcarrierwise insertion for LFDMA and B-IFDMA and, thus, an error floor occurs.

The application of PP leads to the same relative behaviour for LFDMA, IFDMA and B-IFDMA for all data rates. The application of PP to CE with symbolwise pilot insertion improves the SNR-degradation up to 1.5 dB for all three schemes. In general, it can be said that the higher the data rate the better the improvement due to PP [8]. The application of PP to CE with subcarrierwise pilot insertion leads to an improvement of BER, but with increasing SNR, the BER degrades. With increasing SNR, an error floor arises and the BER converges to the curve for CE with interpolation and without PP for high SNR.

If the results in Section 5 for pilot symbol overhead are taken into account, it can be seen, that IFDMA, on the one hand, loses 0.09 dB compared to LFDMA and B-IFDMA. On the other hand, for high SNR-values, better results can be achieved with CE with symbolwise pilot insertion as there is no error floor occuring. At BER=10^{-4}, for IFDMA with symbolwise pilot insertion and without PP the SNR-degradation is 1 dB lower than for LFDMA and B-IFDMA with subcarrierwise pilot insertion. If PP is applied, this effect is even intensified.

7. CONCLUSION

In this paper, LFDMA, IFDMA and B-IFDMA have been compared in terms of pilot insertion for CE. The influence of pilot insertion on CE performance, PAPR, pilot symbol overhead and the practicability of PP applied on the estimated CIR has been investigated for all three schemes. It has been shown that the three schemes show the same behaviour for all data rates if CE with symbolwise pilot insertion is performed. The application of PP leads to the same improvements for LFDMA, IFDMA and B-IFDMA for symbolwise and subcarrierwise pilot insertion. It has also been shown, that IFDMA requires a slightly higher pilot symbol overhead than LFDMA and B-IFDMA for a wide range of data rates due to missing interpolation. The CE performance suffers for high SNR due to interpolation for MMSE independently from the application of PP and the PAPR increases for subcarrierwise pilot insertion. Thus, it can be said that good CE performance and a low PAPR can be achieved especially for high SNR with symbolwise pilot insertion with the drawback of a slightly higher pilot symbol overhead that can be neglected with regard to performance gain.

REFERENCES

[1] N. Benvenuto and G. Cherubini. *Algorithms for Communications Systems and their Applications*. John Wiley & Sons Ltd., 2002.

[2] K. Fazel and S. Kaiser. *Multi-Carrier and Spread Spectrum Systems*. John Wiley & Sons, Ltd., 2003.

[3] T. Frank, A. Klein, E. Costa, and A. Kuehne. Low Complexity and Power Efficient Space-Time-Frequency Coding for OFDMA. In *Proc. of 15th Mobile & Wireless Communications Summit*, Mykonos, Greece, June 2006.

[4] T. Frank, A. Klein, E. Costa, and E. Schulz. Robustness of IFDMA as Air Interface Candidate for Future Mobile Radio Systems. In *Advances in Radio Science*, Miltenberg, Germany, Oct. 2004.

[5] T. Frank, A. Klein, E. Costa, and E. Schulz. IFDMA - A Promising Multiple Access Scheme for Future Mobile Radio Systems. In *Proc. PIMRC 2005*, Berlin, Germany, Sep. 2005.

[6] D. Galda, H. Rohling, E. Costa, H. Haas, and E. Schulz. A Low Complexity Transmitter Structure for OFDM-FDMA Uplink Systems. In *Proc. IEEE Vehicular Technology Conference*, pages 1737–1741, Birmingham, United Kingdom, May 2002.

[7] J. Lim, H. G. Myung, and D. J. Goodman. Proportional Fair Scheduling of Uplink Single-Carrier FDMA Systems. In *Proc. of PIMRC06*, Helsinki, Finland, September 2006.

[8] A. Sohl, T. Frank, and A. Klein. Channel Estimation for DFT precoded OFDMA with blockwise and interleaved subcarrier allocation. In *Proc. International OFDM Workshop 2006*, Hamburg, Germany, August 2006.

[9] A. Sohl, T. Frank, and A. Klein. Channel Estimation for Block IFDMA. In *Proc. International Multi-Carrier Spread Spectrum Workshop*, Herrsching, Germany, Mai 2007.

[10] U. Sorger, I. De Broeck, and M. Schnell. IFDMA - A New Spread-Spectrum Multiple-Access Scheme. In *Proc. ICC'98*, pages 1013–1017, Atlanta, Georgia, USA, June 1998.

[11] B. Steiner. *Ein Beitrag zur Mobilfunk-Kanalschaetzung unter besonderer Beruecksichtigung synchroner CDMA-Mobilfunksysteme mit Joint Detection*. PhD thesis, Universitaet Kaiserslautern, Fortschrittsberichte VDI, Reihe 10, Nr. 337, Duesseldorf: VDI Verlag, 1995.

[12] E. UMTS. *TR-101 112, V3.2.0*. Sophia-Antipolis, France, April 1998.

[13] R. van Nee and R. Prasad. *OFDM for Wireless Multimedia Communications*. Artech House, 1st edition, 2000.

[14] WINNER. Final report on link level and system level channel models. Technical Report D5.4 v. 1.4, WINNER-2003-507581, November 2005.

[15] WINNERII. The winner 2 air interface: Refined multiple access concepts. Technical Report D4.6.1, WINNER II-4-027756, November 2006.